SKBF
KBS
TEKNISK
RAPPORT
82-19

Corrosion of steel in concrete

Carolyn M Preece

Korrosionscentralen
Glostrup, Denmark, 1982-10-14

SVENSK KÄRNBRÄNSLEFÖRSÖRJNING AB / AVDELNING KBS

POSTADRESS: Box 5864, 102 48 Stockholm, Telefon 08-67 95 40

CORROSION OF STEEL IN CONCRETE

Carolyn M Preece

Korrosionscentralen
Glostrup, Denmark, 1982-10-14

A list of other reports published in this series during 1982, is attached at the end of this report. Information on KBS technical reports from 1977-1978 (TR 121), 1979 (TR 79-28), 1980 (TR 80-26) and 1981 (TR 81-17) is available through SKBF/KBS.

CORROSION OF STEEL IN CONCRETE

Report to SKBF, 1982.10.14.

Carolyn M. Preece

Korrosionscentralen

SUMMARY

A comparative study has been made of those properties of Massiv and Standard cements which are considered to determine their ability to protect steel reinforcement from corroding. Saturated Massiv cement has a higher evaporable water content, but a significantly finer pore structure than has saturated Standard cement. This fine structure resulted in an electrical resistivity ten times higher and chloride diffusivity ten times lower than those of Standard cement. Electrochemical measurements have shown that the passive current density of steel in Massiv mortar is higher than that of steel in Standard mortar, but the higher current should lead to a more rapid decrease in potential to a level at which neither chloride attack or hydrogen evolution will occur. Whereas steel in Standard mortar was found to be highly susceptible to crevice corrosion, no such attack has been observed in Massiv mortar. Moreover, the initiation of chloride induced corrosion and the subsequent rates of corrosion were both lower in Massiv mortar than in Standard mortar.

Thus, it may be predicted that Massiv cement would provide greater protection for steel reinforcement in underground structures exposed to chloride containing ground water than would Standard cement.

CORROSION OF STEEL IN CONCRETE

FINAL REPORT, 1982.10.14.

Carolyn M. Preece

INTRODUCTION

A reinforced concrete storage system for radioactive waste material is planned for construction 50 m below the sea bed under a 10 m depth of water. The construction will, therefore, be exposed to salt water and will be in an anaerobic environment after a period of time. The purpose of this project, which was carried out over the six month period 1981.11.01 - 1982.05.31, was to make a comparative study of those properties of "Massiv" cement (a 65% blast furnace slag cement) and "Standard" cement (an ordinary Portland cement) which are considered to determine the cement's ability to protect steel reinforcement from corroding. The properties investigated were electrical resistivity, chloride ion diffusion rates, porosity and the electrochemical behaviour in various environments.

It is not possible to predict the behaviour of "Massiv" cement from previous studies of blast furnace slag (BFS) cements because of the inherent differences in slags obtained from different sources and the different quantities of slag in the cements. However, a survey of the studies that have been made of the corrosion of steel in BFS cements indicates little difference in the protective qualities of BFSC and OPC. OPC. Specifically, Ost and Monfore[1] concluded, on the basis of a visual inspection of the surface of steel bars which had been embedded in either OPC or in BFSC for one year, that there was no noticable

difference between them. Fulton[2] also reported little difference in corrosion rates of steel in the two types of concrete if the concrete cover was less than 3.75 cm. However, for samples with larger cover, seven years' exposure to alternate cycles of drying and salt spray resulted in failure of only 18.7% of the BFSC samples compared with 45.2% of OPC samples. In contrast, Tuutti[3] has found a lower Cl ion threshold for corrosion of steel in "Massiv" cement than in OPC which implies a shorter incubation period before corrosion is initiated. He also concluded that there were no differences in the subsequent corrosion rates of steel in the two cements.

The relatively minor effects of the slag cement on the corrosion of embedded steel are somewhat surprising in view of the significantly finer structure which is thought to be characteristic of the slag cements[4]. However, good quality OPC itself provides excellent corrosion protection for steel and it is probable that the corrosion levels in the laboratory samples of both OPC and BFSC used in these studies were so low as to be visually indistinguishable in the normal, short term laboratory experiments. The electrochemical technique used in the present project, on the other hand, is able to distinguish small differences in corrosion behaviour and has revealed significant differences between the two types of cement.

PREPARATION OF SAMPLES

Table I gives the composition and properties of each of the cements investigated, namely "Standard", an Ordinary Portland Cement and "Massiv", a cement containing 65% blast furnace slag and 35% OPC. For the electrical resistivity, chloride diffusion and porosity measurements, cement pastes with a water/cement (w/c) ratio of 0.5 were used. Electrochemical measurements were made on mortar samples with a water: cement:sand ratio of 0.50:1.00:3.00. The sand used was 0-4 mm quartz sand.

After mixing and casting, the samples were compacted by vibration and stored at 100% RH for 24-48 hrs. Their subsequent treatment is described in each section below.

ELECTRICAL RESISTIVITY

Many recent measurements of electrical resistivity of cement and concrete have employed a.c. techniques because it is thought [5-7] that electrochemical polarization at the electrodes introduces an error into d.c. data. However, studies [8] of resistivities measured at different frequencies and amplitudes indicate that, in fact, the current does not reach its stable level in cement or concrete within the period of the normally employed frequencies (50-1000 Hz). Consequently, a d.c. method was developed in collaboration with Inge Hansson at the Technical University of Denmark. In this technique, the steady state current, I, is determined as a function of applied voltage, V, and the resistance, R, is determined from the slope of the V/I plot.

Two samples of "Massiv" paste and two of "Standard" paste were cast into 11 x 8 x 6 cm moulds and two 3 x 3 cm perforated steel electrodes, spot welded onto steel rods, as shown in Fig. 1, were embedded approximately in the centre of the samples 1 cm apart. The samples were kept at 22°C and 100% RH and the resistivities were determined periodically over a period of 210 days and are given in Fig. 2.

Firstly, it should be noted that the resistivity of the "Massiv" cement is approximately an order of magnitude higher than that of the Standard cement. Secondly, the latter becomes almost constant after one month whereas the "Massiv" continues to increase in resistivity over the whole period investigated (seven months). After this period, the samples were sectioned and the electrodes examined to determine if there were any detectable corrosion. In neither case was there any observable attack of the electrodes.

TABLE I

Composition and properties of "Massiv" and "Standard" cements

Chemical Analysis	Massiv		Standard
CaO	47.5 %		63.7 %
SiO_2	28.5		19.8
Al_2O_3	7.8		4.3
Fe_2O_3	1.4		2.0
MgO	6.9		3.6
K_2O	1.1		1.4
Na_2O	0.6		0.3
total S:	1.7	SO_3:	3.5
Loss on ignition	0.4		1.9
Pb	<5 mg/kg		7 mg/kg
Cd	<0.2		<0.2
Tl	<1		<1
Cr	45		45
Cu	9		10
Co	3		5
Ni	7		10
V	<10		<10
Zn	80		110
Hg	0.04		0.05
	Strength, MPa		
7 day	21		19
14 days	28		34
28 days	35		41
91 days	45		50

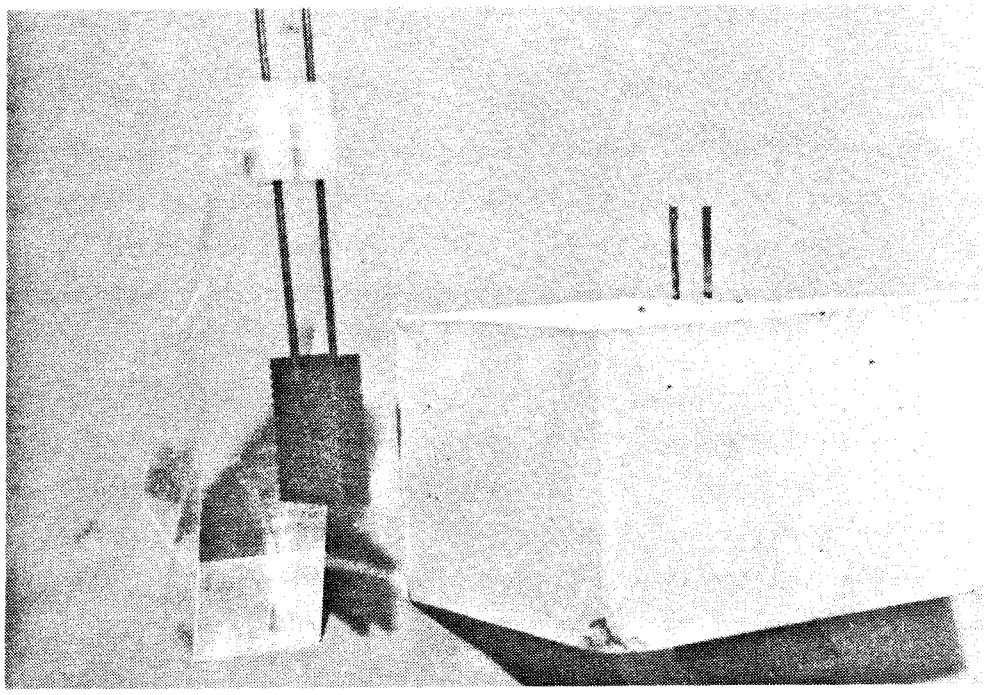

Fig. 1. Paste sample for resistivity measurements. Two mild steel electrodes, shown at left, are embedded in the cement block.

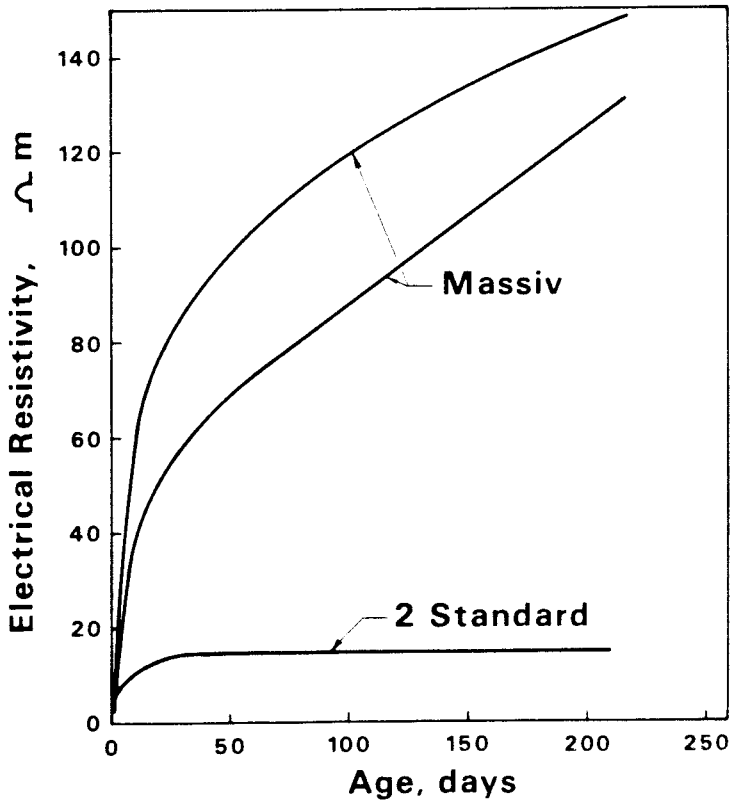

Fig. 2. The electrical resistivities of Massiv and Standard pastes at 22°C and 100% RH.

CHLORIDE DIFFUSION MEASUREMENTS

Cement paste bars for diffusion measurements were cast into 4.5 cm ø tubes and kept under water for six weeks. Three slices of each cement, 2 - 3 mm in thickness, were cut from the bars using a diamond cut-off wheel and were ground to give flat, parallel faces. The slices were then held with silicone glue between two cells as shown in Fig. 3. Both cells were filled with 22.5 ml saturated $Ca(OH)_2$ solution and NaCl was added to one cell to give a 1 M solution. The cells were kept at room temperature and, periodically, 0.1 ml of solution was removed from the second cell and analysed using an Orion Model 96-17 chloride electrode. Measurements were also made by spectrophotometry but this technique proved to be less sensitive than the chloride electrode at the lower chloride concentrations (<100 ppm). The experiment was repeated at 40°C and 50°C on five samples of each paste and the results are shown in Figs. 4-6.

At all three temperatures, chloride was detected in the second cell of the "Standard" samples within the first 24 hours whereas there was a significant period before any detectable chloride concentration was observed through the "Massiv" samples. At room temperature, this "incubation period" was almost two months. It is probable, therefore, that the chloride diffusing into the cement during this period is being chemically bound to the cement whereas there is much less chemical reaction between the chloride and the "Standard" cement. The "incubation period" is reduced to approx. 5 days at 40°C and 2-3 days at 50°C but it is still evident.

The effective diffusion coefficients, D, determined according to Fick's 1st. Law, were calculated from the slopes of the plots in Figs. 4-6 and are given in Table II. The values of log D are plotted versus the reciprocal of the absolute temperature in Fig. 7. For the "Standard" paste the data can be considered linear and an activation energy of 40.8 kJ/mole is obtained from the slope of the plot. This compares well with the value obtained by Page et al.[9] of 44.6 kJ/mole for OPC with w/c = 0.50. The data for "Massiv", on the other hand, is not linear and suggests that more than one process is operative in this temperature range. This behaviour may be a result of a chemical binding, as suggested above.

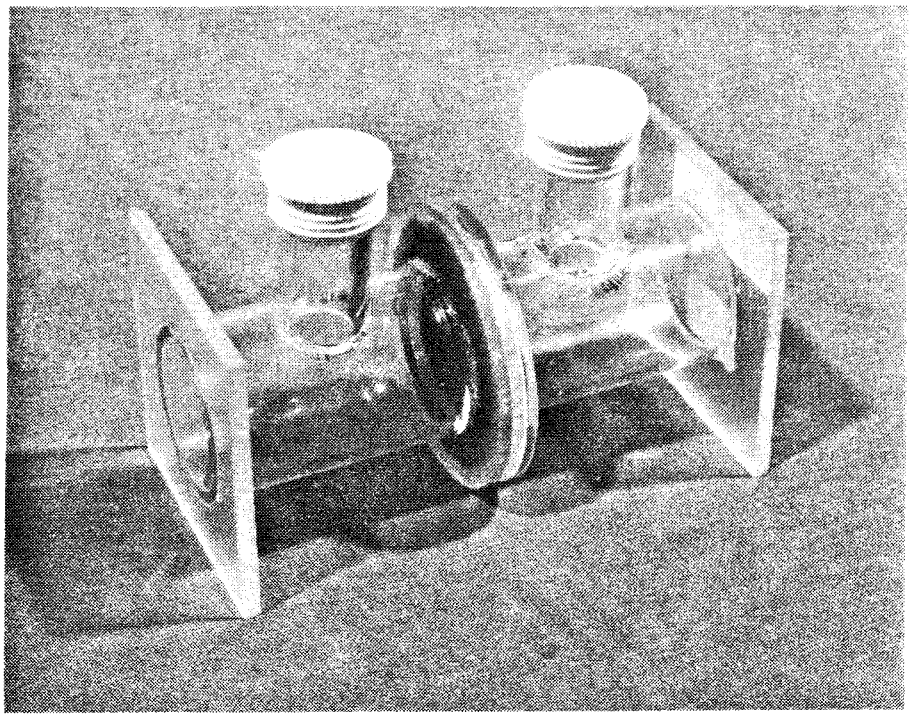

Fig. 3. Chloride diffusion cell

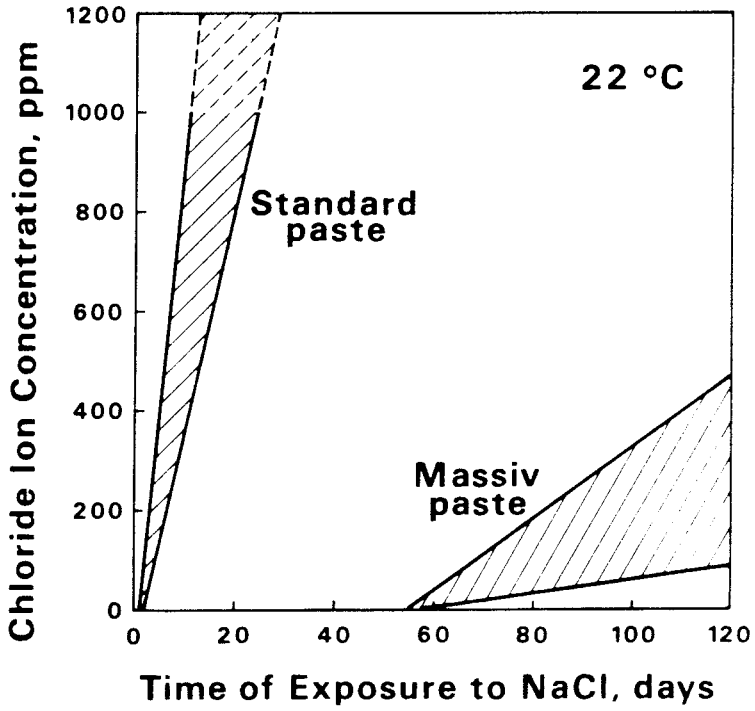

Fig. 4. Chloride ion diffusion through "Massiv" and "Standard" cement pastes at 22°C.

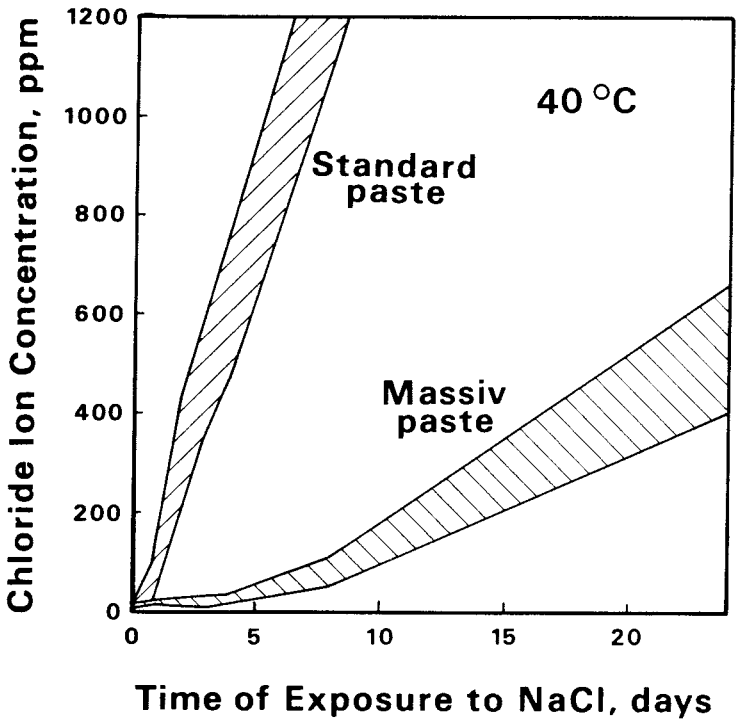

Fig. 5. Chloride ion diffusion through "Massiv" and "Standard" cement pastes at 40°C.

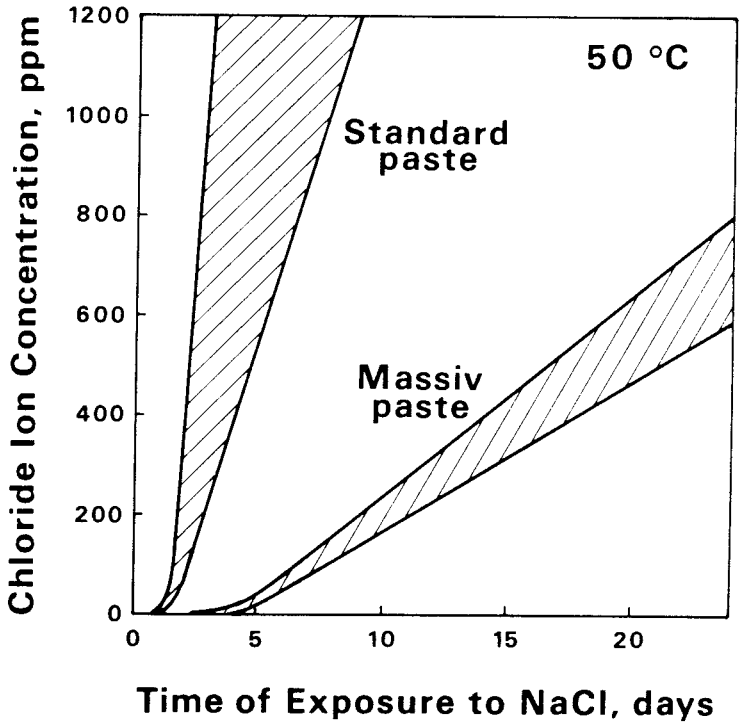

Fig. 6. Chloride ion diffusion through "Massiv" and "Standard" cement pastes at 50°C.

TABLE II

Effective diffusion coefficients, D, and activation energies, E , for chloride ions in different cement pastes and mortars.

Material	W/C	T°C	D, 10^{13} m^2/s	E, kJ/mole	Ref.
Massiv paste	0.50	22	0.5-3.0		present
" "	"	40	9.7-16.5		"
" "	"	50	12 - 18		"
Standard paste	"	22	22 - 44		"
" "	"	40	69 - 78	40.8	"
" "	"	50	72 - 350		"
OPC paste	"	7	18.6-22.3		9
" "	"	13.5	14.7-31.7		"
" "	"	25	40.6-48.2	44.6	"
" "	"	45	152 - 201		"
BFSC paste	"	25	4.1		"
OPC mortar	"	22	29.6		4
BFSC mortar	"	22	0.4		"

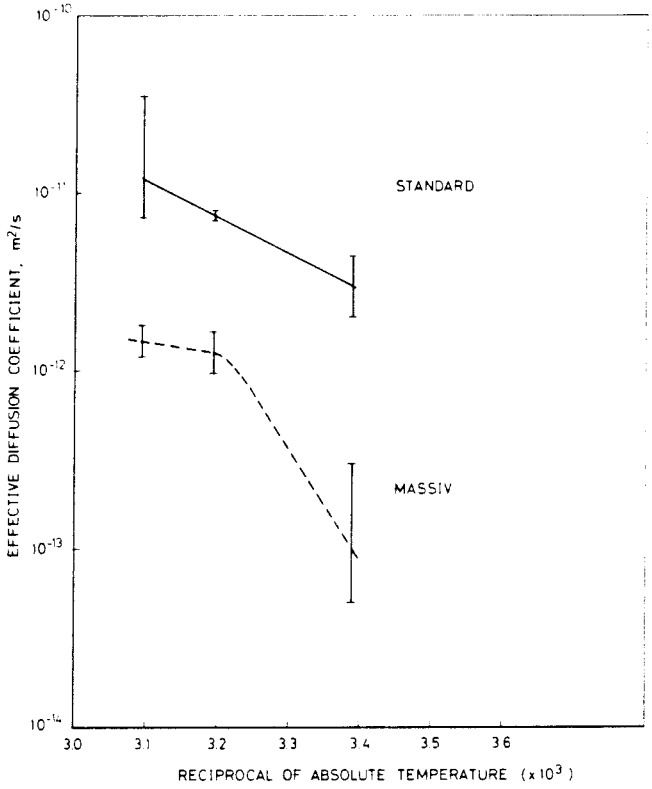

Fig. 7. The effective chloride diffusivities as a function of reciprocal temperature for "Massiv" and "Standard" pastes.

POROSITY AND PORE SIZE DISTRIBUTION

The higher resistivity and lower diffusion rates in "Massiv" cement suggest that it has a lower porosity and/or a finer pore distribution than has "Standard" cement. In order to obtain some quantitative measure of these parameters, low temperature microcalorimetry measurements[10] of the two cements have been made in collaboration with Dirch Bager at the Technical University of Denmark. In this technique, the heat flow resulting from freezing is measured during cooling the samples from 0°C down to -55°C. The lower freezing temperatures correspond to smaller pore sizes and an estimate of the total porosity can be made from the area under the curves shown in Fig. 8.

The narrow peak at -4°C, particularly evident in the "Massiv" sample, is attributed to "free" water on the surface or in large casting pores. The freezing of water in the structural pores of the cement pastes be-

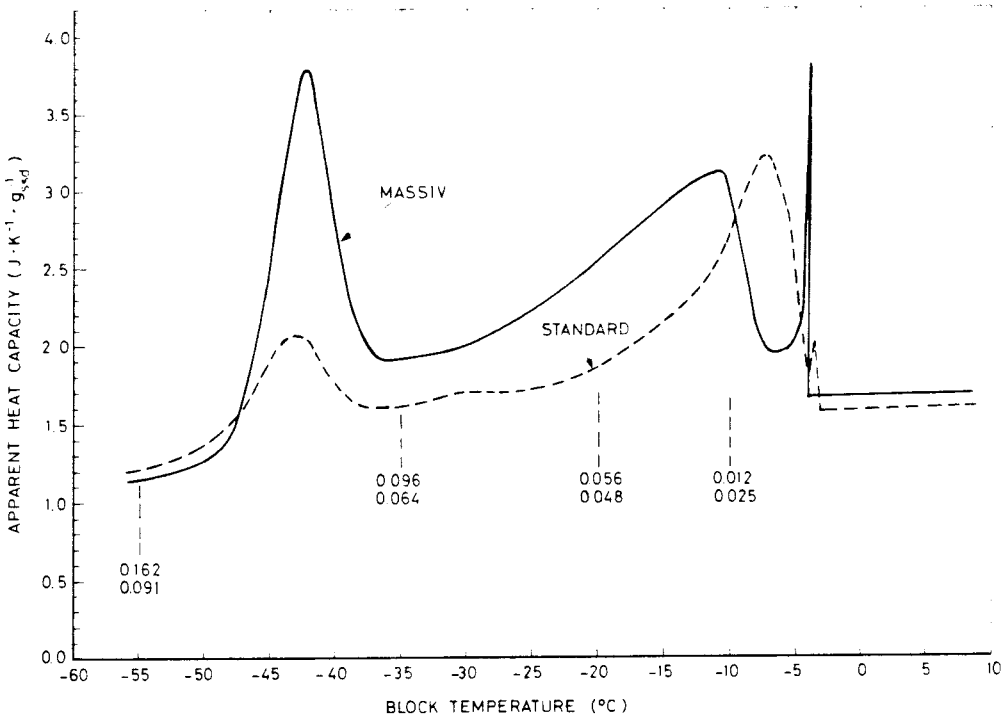

Fig. 8. The apparent heat capacities of Massiv and Standard pastes as a function of cooling temperatures.

gins -5°C in the "Standard" and -8°C in the "Massiv". The pores responsible for this freezing, which are essentially the largest structural pores in the cement gel, have diameters of approximtely four times larger in "Standard" than in "Massiv". Two major differences in the data for the two cements are (i) the heights of the peaks at ∿-43°C and (ii) the total areas under the curves. The significantly larger low-temperature peak in the "Massiv" cement indicates a very much higher density of fine pores (in the 20Å range). The areas under the curves show that the "Massiv" has a greater evaporable water content than the "Standard". This was also shown by drying samples under vacuum at 92°C: the evaporable water contents of "Massiv" and "Standard" pastes were found to be 0.339 and 0.279 g(water)/g(dry cement paste), resp.

In Fig. 8, the figures at -10 , -20 , -35 and -55°C correspond to the cumulative amount of water that has frozen at that temperature in g(water)/g(dry cement paste), the upper figures being the values for "Massiv" and the lower ones for "Standard". Thus, it is obvious that the excess water in the "Massiv" paste is present in the fine pore structure. It should also be noted that only 47% of the total evaporable water in "Massiv" and 32% of that in "Standard" is freezable. The remaining water is present in a form that does now allow it to freeze.

The higher free water content of the "Massiv" cement may be attributed to the fact that the slag requires less water for hydration than does "Standard". The finer structure is probably due to the fact that because there are two different types of reactive particles in the original mix, there is a chemical driving force for the hydration reactions to take place throughout the space between the particles[11]. In "Standard" cement, in which all the clinker particles have approximately the same composition and chemical potential, there is no such driving force and the hydration will occur preferentially close to the clinker particles, leaving larger spaces (pores) between the hydration products. Thus, the average pore size in the "Standard" cement is larger although the total pore volume is lower than in the "Massiv". Therefore, it may be concluded that, although there is little chemical difference in the two pastes, there is a significant difference in their physical structure.

ELECTROCHEMICAL REACTIONS

For an electrochemical reaction to occur (in the absence of an external source of electrical energy) there must be two half cell reactions: one capable of producing electrons (the anodic half cell reaction) and one capable of consuming electrons (the cathodic half cell reaction). Moreover, the rates of production and consumption must be equal or the reaction will cease.

For steel embedded in concrete, the anodic half cell reactions of interests are

$$3Fe + 4H_2O \rightarrow Fe_3O_4 + 8H^+ + 8e^- \qquad \text{Eq. 1a}$$

$$2Fe + 3H_2O \rightarrow Fe_2O_3 + 6H^+ + 6e^- \qquad \text{Eq. 1b}$$

$$Fe \rightarrow Fe^{++} + 2e^- \qquad \text{Eq. 1c}$$

For good quality concrete in which the pore water typically has a pH $\sim$13.5, Eq. 1a is the principal reaction of interest.

The possible cathodic half cell reactions depend on the availability of O_2 and on the pH. The most likely ones are:

$$2H_2O + O_2 + 4e^- \rightarrow 4OH^- \qquad \text{Eq. 2}$$

$$2H^+ + 2e^- \rightarrow H_2 \qquad \text{Eq. 3}$$

The possibility of these reactions occurring depends on the pH of the environment (in concrete, this is the pH of the pore water) and on the electrochemical potential, E, existing at the steel surface. One can determine theoretically whether or not the reaction is thermodynamically possible but, unfortunately, one can only determine their kinetics (the rate of corrosion) empirically.

The values of E as a function of pH for which the above reactions are in equilibrium can be determined from the Nernst equations and plotted as in Fig. 9 .

At pH = 13.5, iron is in equilibrium with Fe_3O_4 at E = -1125 mV on the standard calomel electrode (SCE) scale (-881 mV on the standard hydrogen electrode (SHE) scale). In order for corrosion to occur, the potential at the steel surface must be more positive than this value and, in theory, the more positive the potential is than -1125 mV, the higher will be the corrosion rate. However, at high pH (>9) in the presence of O_2, iron forms a passive film on its surface. This film acts as a protective coating but is not completely protective. Thus, corrosion is not stopped but the rate of corrosion is significantly reduced. A second effect of this passive film is that there is no unique corrosion potential: in aerated concrete, the potential of the steel may be anywhere from +186 to -644 mV SCE (+430 to -400 mV SHE)[12a] and the steel will still be passivated. The greater the supply of O_2, the higher the potential is likely to be within this range. The potential cannot increase to a value higher than the equilibrium potential (+186 mV SCE (Line (b) in Fig. 1)). Moreover, the rate of O_2 reduction diminishes rapidly as this value is approached.

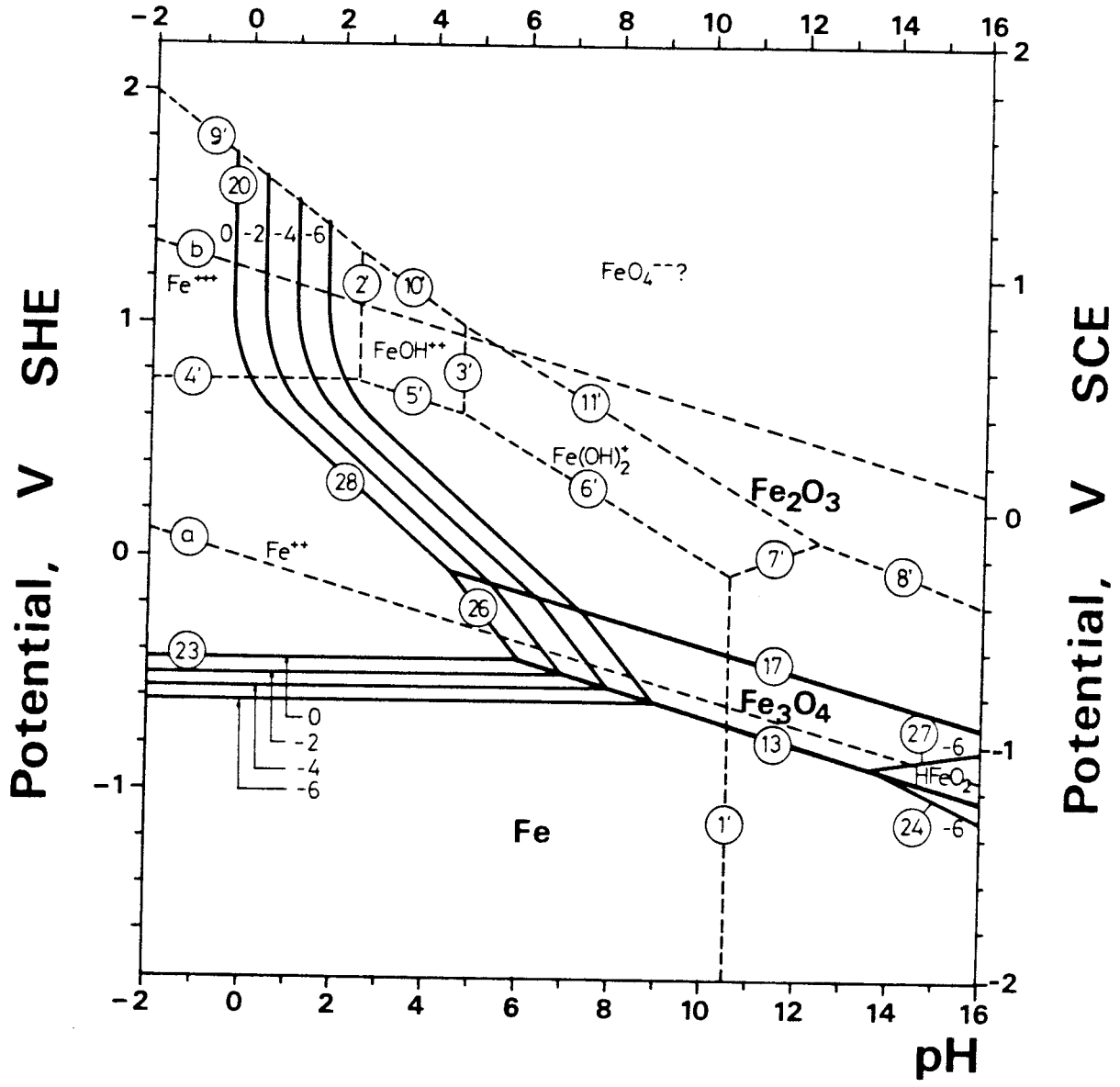

Fig. 9. The potential - pH equilibrium diagram for the system iron-water at 25°C (ref. 12).

One can, thus, predict the following sequence of events when steel is embedded in concrete in the proposed project.

1. The steel is cast into wet cement and rapidly develops a passive surface film due to the high pH of the pore water and the availability of oxygen. The potential of the steel may lie anywhere between approx. +186 to -644 mV SCE: it may be stable or it may fluctuate with time. In the absence of aggressive factors such as carbonation or chloride ion attack, the corrosion current will be low, probably of the order of 10^{-4} - 10^{-3} A/m^2 (0.1-1.0 µm/yr).

2. It should be noted that maintenance of the passive film requires both a high pH (>9) and access of oxygen. The greater the availability of oxygen, the thicker will be the passive film and the higher (more positive) will be the corrosion potential, E_R.

3. When the concrete is buried below ground, the availability of oxygen will diminish and eventually all the oxygen existing in the concrete will be reduced by the (slow) corrosion reaction.

4. When all the available oxygen has been consumed, the potential will drop to a level at which the passive film is not stable (ie < -644 mV SCE) and the film itself will be reduced, leaving the bare steel in an "active" state. The corrosion rate in this active state will be determined by (a) the potential E_R, (b) the diffusion rates of reactants and corrosion products in the concrete and (c) the electrical resistivity of the concrete.

5. In the absence of oxygen, the cathodic reaction (whose rate must be equal to the anodic (corrosion) rate) is the evolution of hydrogen. The value of E_R determines the maximum thermodynamically possible hydrogen pressure that can be built up before the corrosion reaction is halted. E_R also determines how much the corrosion reaction is polarized and, therefore, the rate of corrosion. These two factors effectively work in opposition to each other. Thus, if the iron dissolution reaction is strongly polarized (E_R high), the initial corrosion reaction is rapid but the allowable hydrogen pressure is very low and, when this pressure is reached, both reactions (hydrogen evolution and iron corrosion) will stop. If, on the other hand, the polarization is small ($E_R \rightarrow E^{\circ}_{Fe}$) the reaction rates will be extremely low and the allowable hydrogen pressures, although much higher, will take a correspondingly long time to build up. It should also be noted that the hydrogen pressures can only build up if the hydrogen is developed faster than it can diffuse away through the concrete system.

6. The lowest possible value of the potential at pH 13.5 is -1125 mV SCE (-881 mV SHE). At this potential, iron is in equilibrium with Fe_3O_4 and is not corroding and, therefore, there can be no hydrogen evolution. In practise, the potential will lie at a value greater than this and the higher its value, the lower the possible hydrogen pressures according to the equation:

$$E = -0.059\ pH - 0.0295 \log P_{H_2}$$

7. In practise, there have been very few electrochemical measurements of steel in concrete kept under anaerobic conditions. However, those that have been made[13-15] indicate that the available oxygen in the concrete will be consumed over a period of 6 months to 2 years. The lowest reported value of E_R under these conditions is -994 mV SCE (-750 mV SHE) at which the maximum possible pressure

of hydrogen would be 0.03 atm. This potential was obtained after the structure had been in an anaerobic environment for nearly two years and it is possible that lower values could be reached over long periods. It should be emphasised, however, that the lower the potential, the slower is the corrosion rate and the easier it is for the hydrogen to diffuse away before any substantial hydrogen pressure can develop.

EXPERIMENTAL ELECTROCHEMICAL MEASUREMENTS

Determination of polarization curves is a standard and very common procedure in the study of corrosion of metals but has not been widely used for steel in concrete because of the experimental difficulties involved with (a) the very low current densities (b) the "IR drops" due to electrical resistance of the concrete and (c) the long experimental times required. However, such curves can give an estimate of both the actual corrosion rates occurring at the time of the experiment and an idea of how the corrosion rate will change if the corrosion potential, E_R, changes due to, for example, environmental changes. The curves can be readily explained with reference to Fig. 10 which is a schematic representation of the electrochemical reaction rates.

In Fig. 10 the equilibrium potentials for reactions 1a, 2 and 3 are given as E°_{Fe}, E°_{O} and E°_{H}, respectively. At equilibrium in an aerated solution of high pH, the potential will attain that value at which the cathodic current due to oxygen reduction is equal to the anodic current due to iron dissolution or oxidation ($E_{RFe/O}$) and the corresponding corrosion rate will be $i_{RFe/O}$. In deaerated solutions, on the other hand, the corrosion potential, $E_{RFe/H}$ and corrosion current $i_{RFe/H}$ will attain lower values, as shown, corresponding to the values at which the rate of hydrogen evolution is equal to that of iron dissolution.

Because of the large range of current values often involved, the curves are usually plotted on a semilogarithmic scale with anodic and cathodic currents plotted in the same direction, as illustrated in Fig. 11.

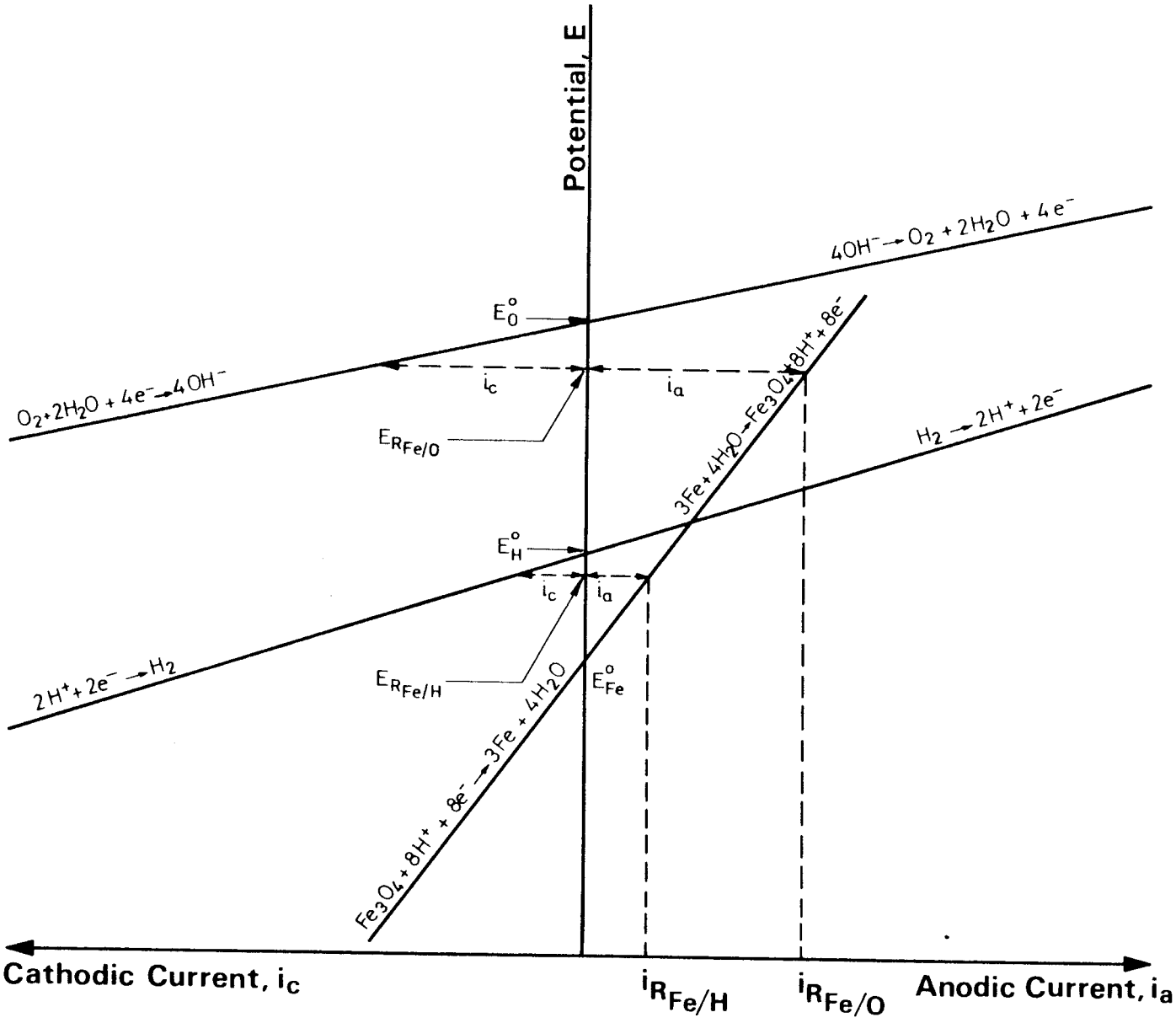

Fig. 10. Schematic representation of the potential-current relationship for Eg. 1a, 2 and 3.

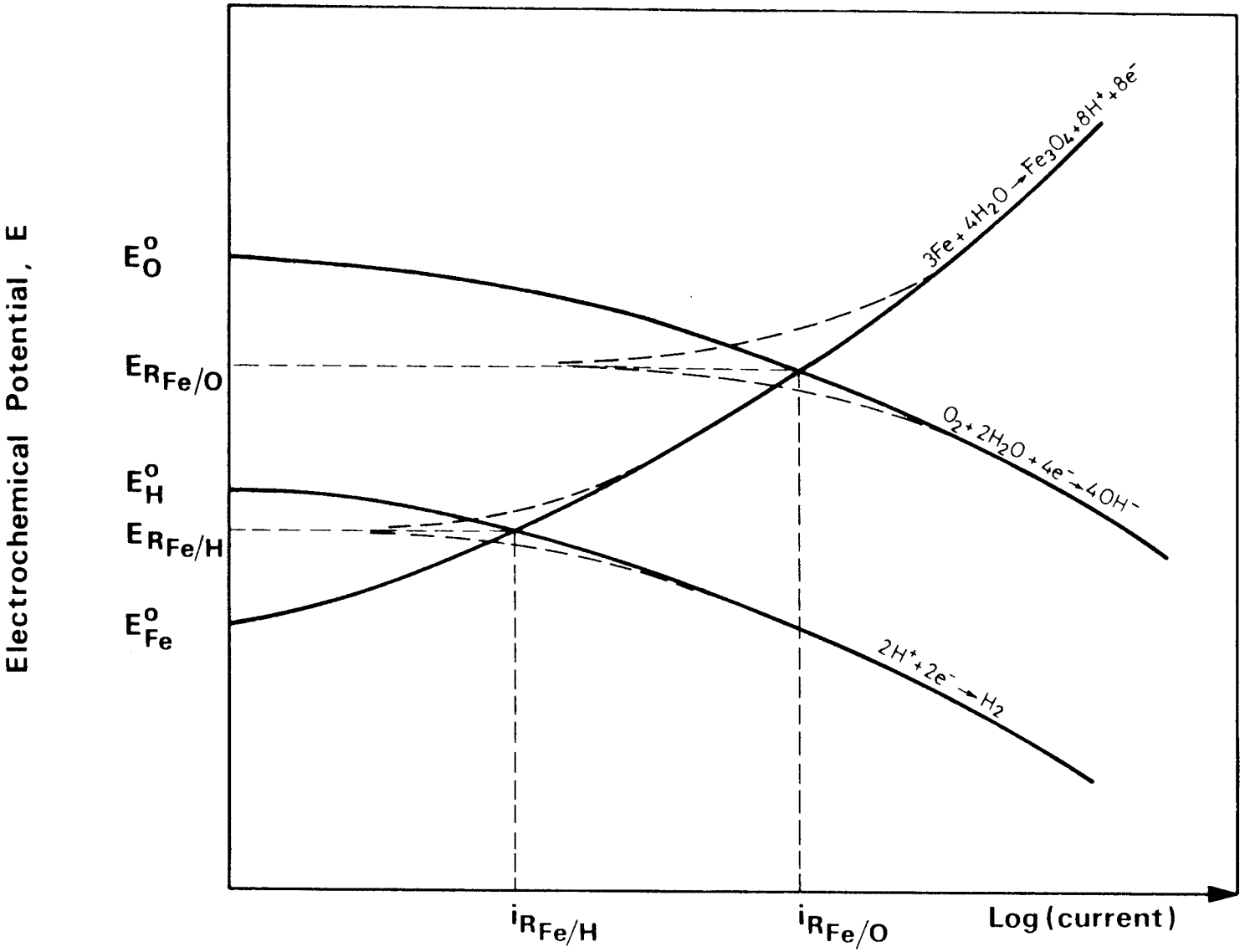

Fig. 11. Schematic representation of the E vs log i relationship for Eg. 1a, 2 and 3.

In practise it is not possible to determine the actual corrosion rate, i_R, directly. This is because, during actual corrosion, the rate of emission of electrons by the iron is exactly equal to the rate of consumption of electrons by the oxygen or hydrogen ions and, therefore, there is no measurable net current. In order to obtain an estimate of the current, it is necessary to shift the potential away from the equilibrium, measure the resultant net current and extrapolate the data to the equilibrium potential.

Experimentally, this is accomplished as illustrated schematically in Fig. 12. A steel rod is embedded in the cement, mortar or concrete, and is immersed in water and held at a constant electrochemical potential with respect to a reference electrode. The current flowing between the embedded steel (the working electrode) and an external steel plate (the counter electrode) is measured. The process is then repeated for different values of applied potential. What one actually measures is the net current ($|i_a|-|i_c|$) shown as heavy dashed lines in Fig. 11.

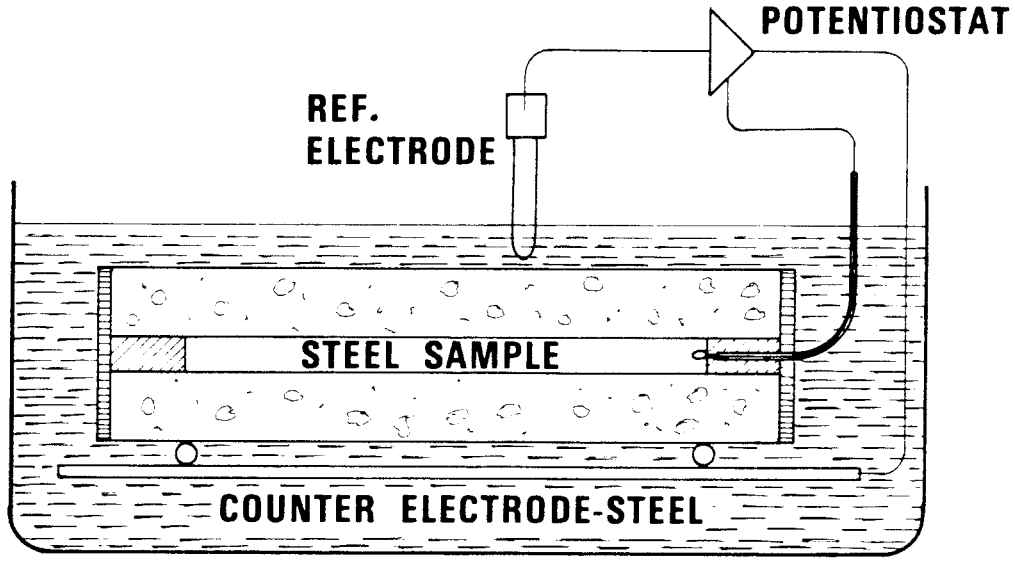

Fig. 12. Schematic diagram of electrochemical cell.

ELECTROCHEMICAL MEASUREMENTS

Two sets of rectangular mortar samples of each cement type were cast on 81.09.04 and were kept immersed in water. One set consisted of 4 x 4 x 16 cm^3 prisms in which are embedded single 8 mm ø mild steel electrodes as illustrated in Fig. 13. The second set had five electrodes, 2 with 5 mm cover, 2 with 10 mm cover and 1 with 15 mm cover. During the hardening period of the samples, air tight, insulated tanks and the electronic potentiostatic control system were constructed. In order to simulate the anaerobic conditions which will prevail underground storage, after four months hardening, the samples were immersed in nitrogen saturated water in three different tanks at 45 C. They were then held at -900 mV vs. standard calomel electrode (SCE) until the current flowing between the samples and an external steel counter electrode (Fig. 12) dropped to $\sim 10^{-4}$ A/m^2 or, in some cases, even became anodic. This condition indicates the absence of oxygen in the cement.

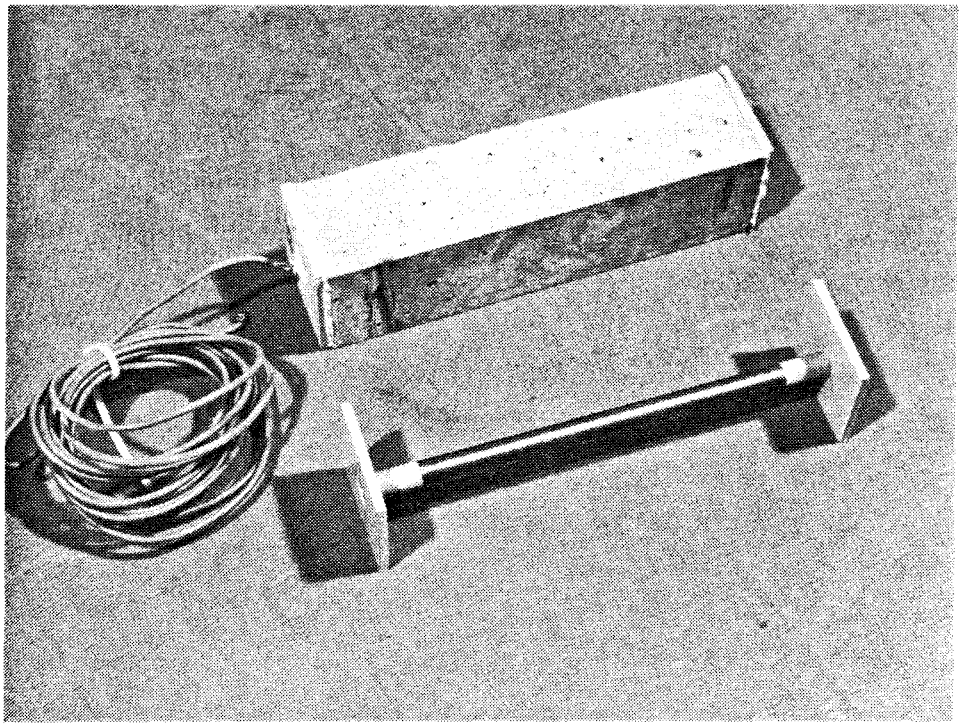

Fig. 13. Mortar sample for electrochemical measurements. A steel electrode with plastic end plates such as that shown in the lower part of the figure, is embedded in the mortar.

Potentiostatic polarization curves for each of the samples were then determined. The potential of the embedded electrodes was held constant with respect to the standard calomel reference electrode (SCE) for 24 hrs. and the current flowing between each sample and the counter electrode was measured. This procedure was repeated for potentials ranging from -1000 mV to +450 mV SCE. It should be noted that the currents were not completely stable after 24 hrs. but time did not permit a longer period for each value of potential and the data are considered reasonable for comparison of the two mortars. The polarization data for four of the single electrode samples of each mortar are plotted in Fig. 14. The remaining samples exhibited similar behaviour to that shown in the figure.

After completion of the polarization curves, NaCl was added to one tank to give a 1 M solution and N_2 was continued to be bubbled through the solution. The nitrogen was replaced by CO_2 in the second tank and by air in the third tank. The samples were then held at an anodic potential (+100 mV SCE) in order to accelerate corrosion initiation and the currents were monitored daily until the effects of Cl were detected as a sharp increase in corrosion current of the "Standard" samples (approximately 3-4 weeks). No change was detected in any of the "Massiv" samples at this time and there was no detectable effect of CO_2 or O_2. A second polarization curve was then determined for each of the samples and the data for the single electrode samples are plotted in Figs. 15-17. The data for the five-electrode samples were similar but the scatter in the data for the "Standard" samples was greater, as illustrated in Fig. 18.

For investigations at 35°C, six additional five-electrode samples of each mortar were cast, hardened for 11 weeks and then held at -900 mV SCE under N_2 saturated water at 35°C until the oxygen in the mortars had been cathodically reduced. Potentiostatic polarization curves were then determined and are plotted in Fig. 19. Two samples of each were then held in (a) deaerated 1 M NaCl, (b) aerated 1 M NaCl and (c) aerated water at +100 mV SCE and, after 2 months, polarization curves were again determined, and are plotted in Figs. 23 and 24.

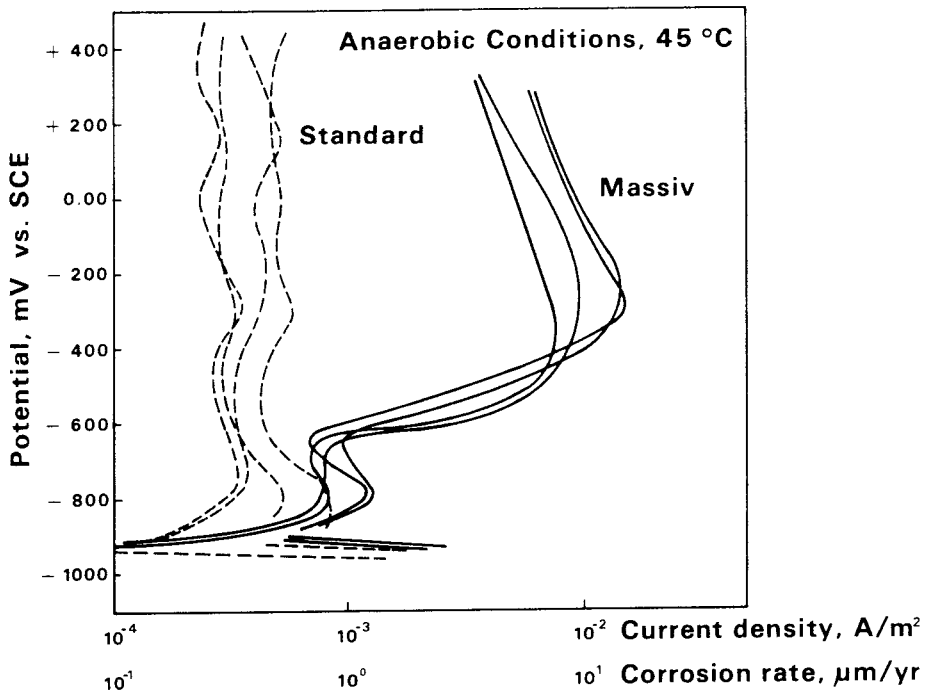

Fig. 14. Electrochemical potentiostatic polarization curves for single steel electrode samples in "Massiv" and "Standard" mortar samples in N_2 saturated water at 45°C.

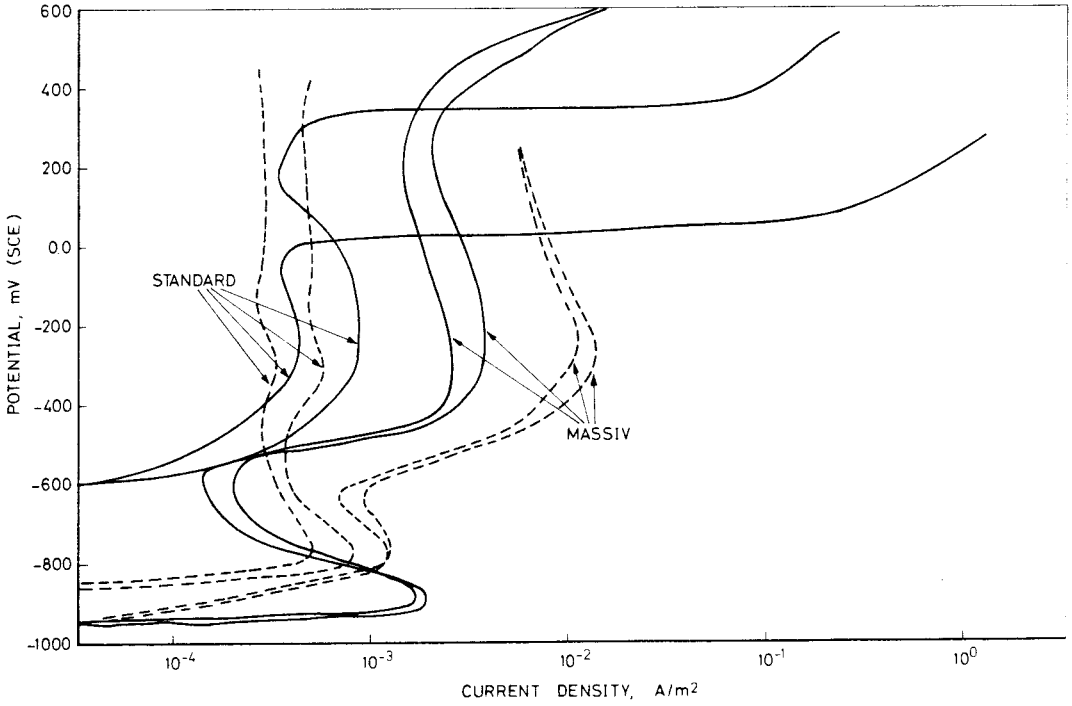

Fig. 15. Electrochemical potentiostatic polarization curves for single steel electrodes in Massiv and Standard mortars at 45°C. The dashed lines are for samples tested in N_2 saturated water and the solid lines are for the same samples subsequently tested in O_2 saturated water.

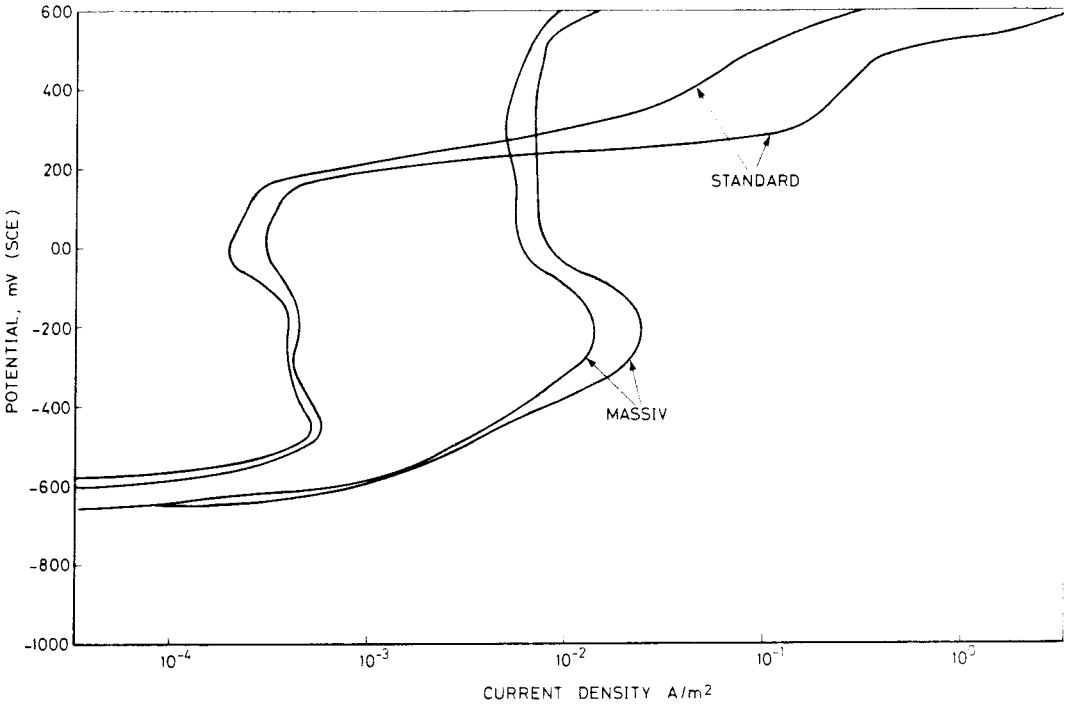

Fig. 16. Electrochemical potentiostatic polarization curves for single steel electrodes in "Massiv" and "Standard" mortars at 45°C in CO_2 saturated water.

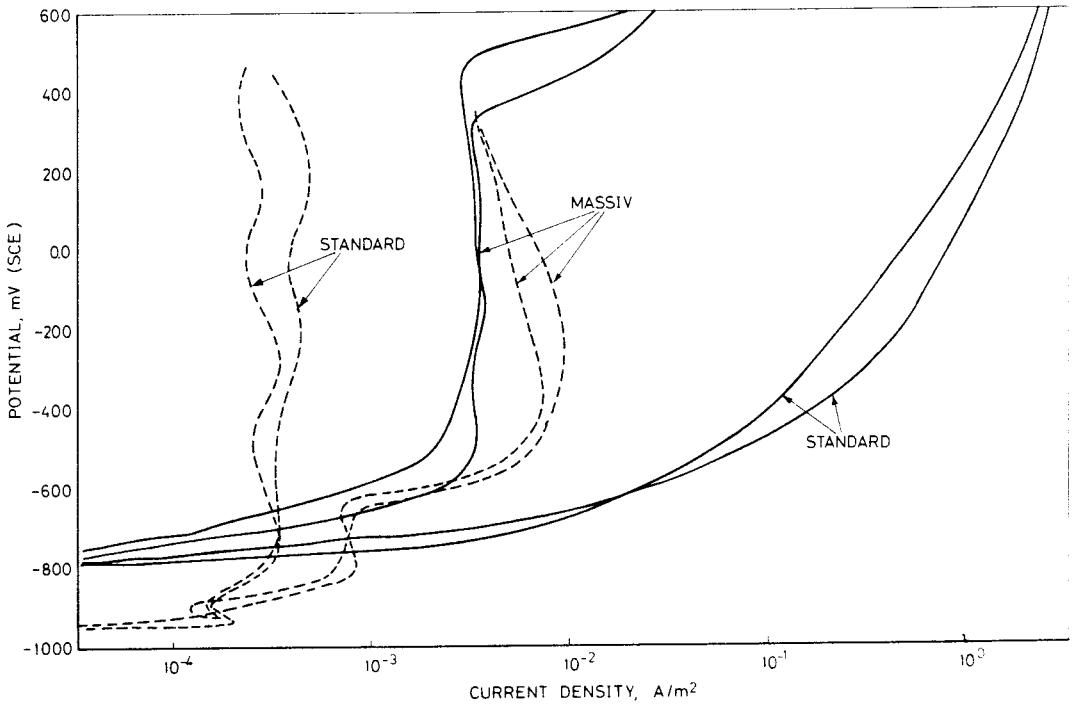

Fig. 17. Electrochemical potentiostatic polarization curves for single steel electrodes in "Massiv" and "Standard" mortars at 45°C. The dashed curves are for samples tested in N_2 saturated water and the solid curves are for the same samples subsequently tested in N_2 saturated 1 M NaCl solution.

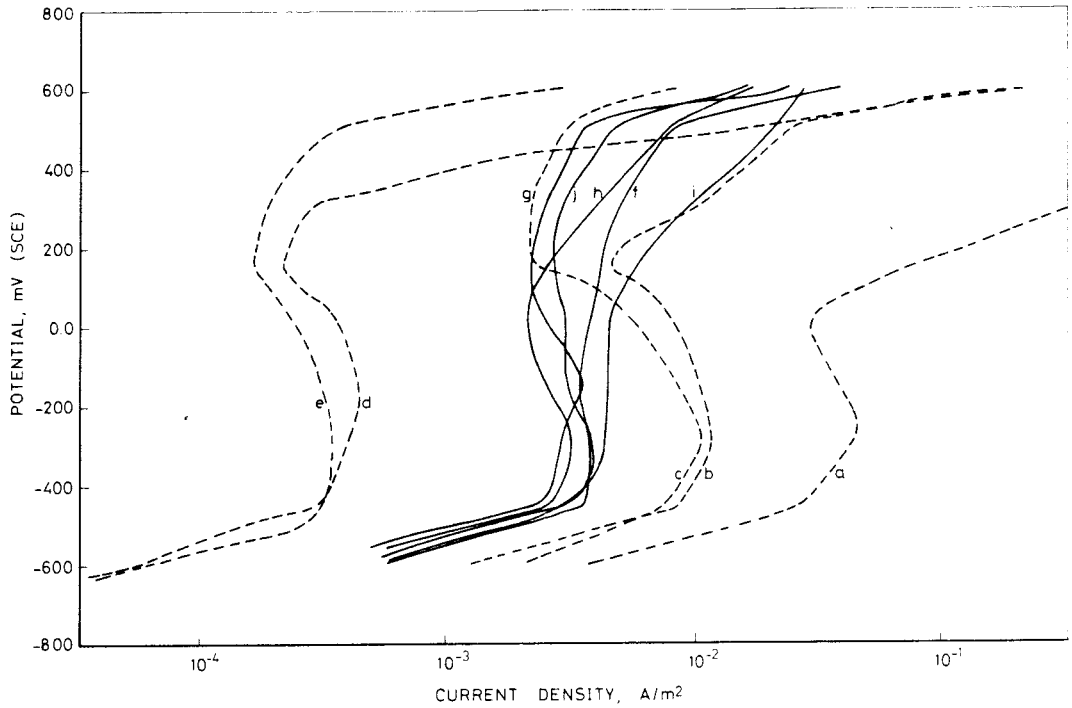

Fig. 18. Electrochemical potentiostatic polarization curves for five-electrode samples tested at 45°C in O_2 saturated water. Dashed curves are for "Standard" mortar with the following covers: (a) and (b) 5 mm, (c) and (d) 10 mm, (e) 15 mm. The solid lines are for "Massiv" mortar with the following covers: (f) and (g) 5 mm, (h) and (i) 10 mm, (j) 15 mm.

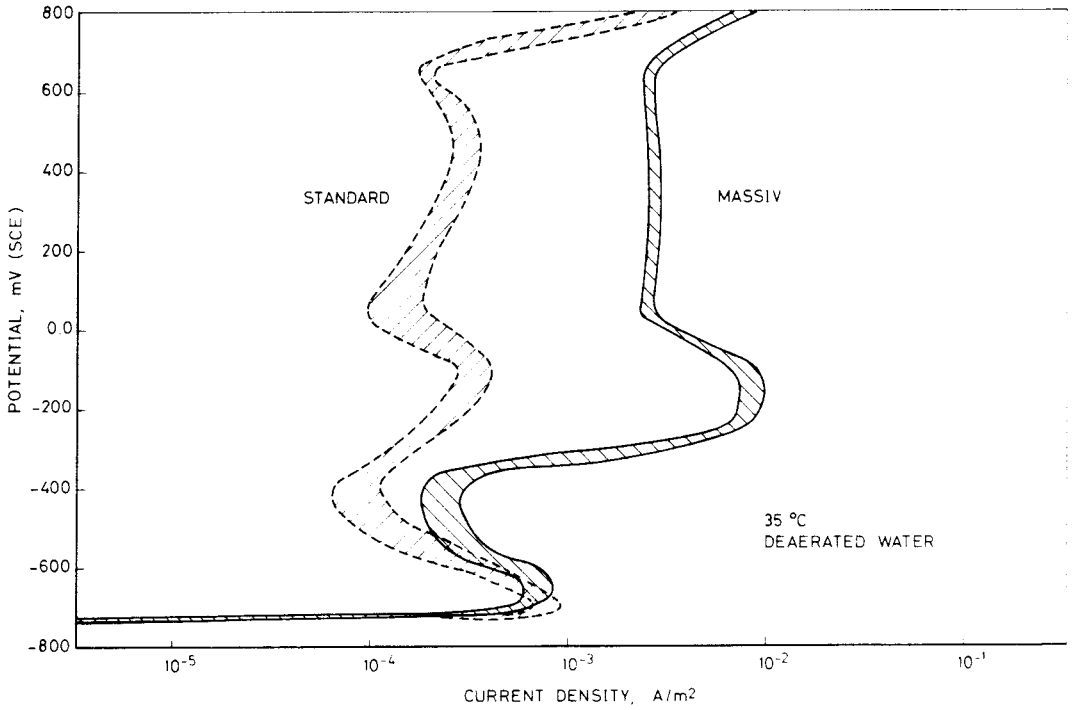

Fig. 19. Electrochemical potentiostatic polarization curves for five-electrode specimens of "Massiv" and "Standard" mortars tested at 35°C in N_2 saturated water.

It is apparent from Figs. 14 and 19 that the passive behaviour of steel om deaerated "Massiv" mortar is quite different from that of steel in deaerated "Standard". Whereas the latter readily passivates with a passive current density of $\sim 5.10^{-4} A/m^2$ at 45°C and $\sim 1.10^{-4}$ A/m^2 at 35°C, the electrodes in "Massiv" have a lower tendency to passivate and have a current density of $\sim 5.10^{-3}$ A/m^2 at both 45°C and at 35°C.

In view of the higher electrical resistivity, lower diffusion rates and finer pore structure of the "Massiv" cement, this behaviour is somewhat surprising but may be explained as follows. Under potential control, the potentiostat absorbs the electrons supplied by the first step in the corrosion reaction:

$$Fe \rightarrow Fe^{++} + 2e^{-}$$

The ferrous ions then react in a series of steps with the pore solution to form a passive film which is thought to eventually consist predominantly of magnetite. In deaerated cement, one of the rate determining reactions in the passive film formation is:

$$Fe^{++} + 2OH^{-} \rightarrow Fe(OH)^{-}$$

It is probable that the above reaction is restricted in "Massiv" cement by the lower availability of hydroxyl ions. This could be due a reduction in the concentration of OH^- ions in the pore water by slag reaction with the alkalis and with $Ca(OH)_2$. Longuet et al. [16] have, in fact, shown a reduction in OH^- concentration in slag cements relative to that in OPC but the available OH^- was more than adequate for passivation. However, the samples considered here were kept at elevated temperatures for long periods and the reaction rate of the slag may have been increased with a corresponding greater decrease in OH^- content.

An second possible explanation, however, is that the dense structure of the mortar limits the diffusion of hydroxyl ions to the steel/cement interface, thereby retarding the formation of the passive film.

Figure 15 shows that the passive current density of steel in aerated "Massiv" mortar is approximately five times lower than that of deaerated samples. This may be a real effect resulting from a more protective passive film. It is, however, probably predominantly due to the cathodic reaction provided by the oxygen. Some of the electrons given up by the iron which, in deaerated cement, would all be registered as current in the measuring circuit, are absorbed by the reaction:

$$O_2 + 2H_2O + 4e^- \rightarrow 4OH^-$$

Apart from this apparent reduction in passive current density, the behaviour of the steel in "Massiv" mortar is not affected by the oxygen or by the applied potential. The steel embedded in "Standard", on the other hand, began to corrode rapidly at potentials greater than 0.0 mV SCE.

Subsequent examination of the electrodes showed that crevice corrosion had been initiated in the steel/plastic interface, as illustrated in Fig. 20. Such corrosion also occurred in "Standard" samples exposed to CO_2 saturated water as is evident from the sudden increases in current densities in Fig. 16 and by the subsequent visual examination, Fig. 20.

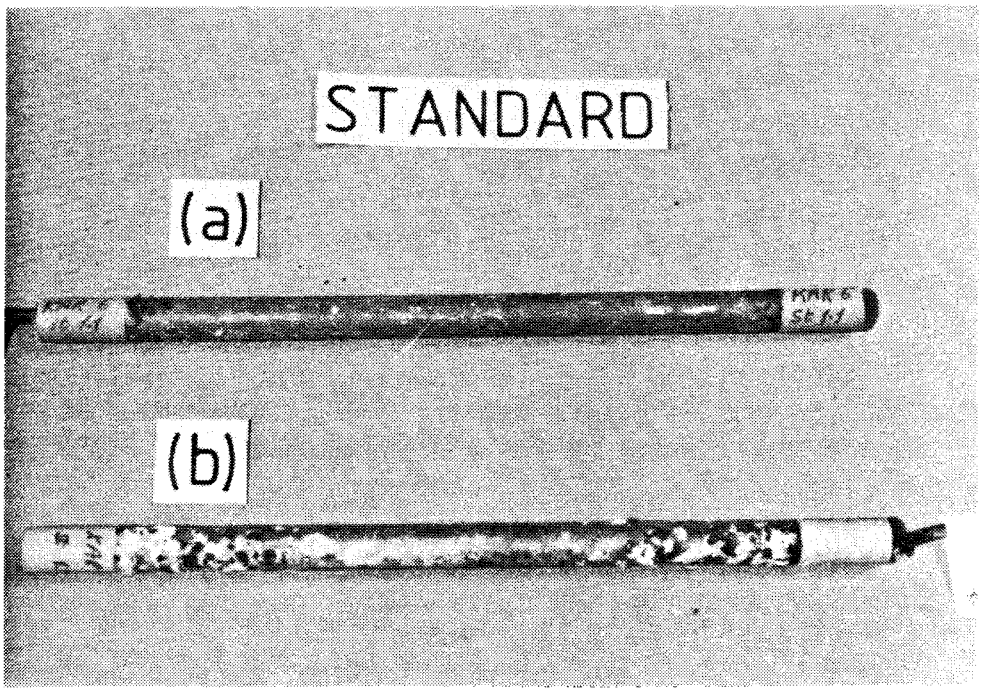

Fig. 20. Electrodes removed from "Standard" mortar after being held in (a) O_2 saturated water and (b) CO_2 saturated water for 8 weeks. Note the crevice corrosion initiated at the interface between the steel and the plastic.

Most investigators who have studied the corrosion of steel in concrete have encountered this problem in laboratory samples and, although the electrode design used in this investigation has proved to be the best of the many tested, it is obviously imperfect. It should be noted, however, that none of the "Massiv" samples has shown any indication of this problem to date. Only one sample exposed to O_2 or CO_2 has been sectioned as yet and there was no evidence of any corrosion. The remaining samples have not shown any sign of such corrosion as yet.

The time of exposure of "Standard" samples to Cl ions before corrosion was detectable, was, as expected, dependent on the cover as shown in Fig. 21.

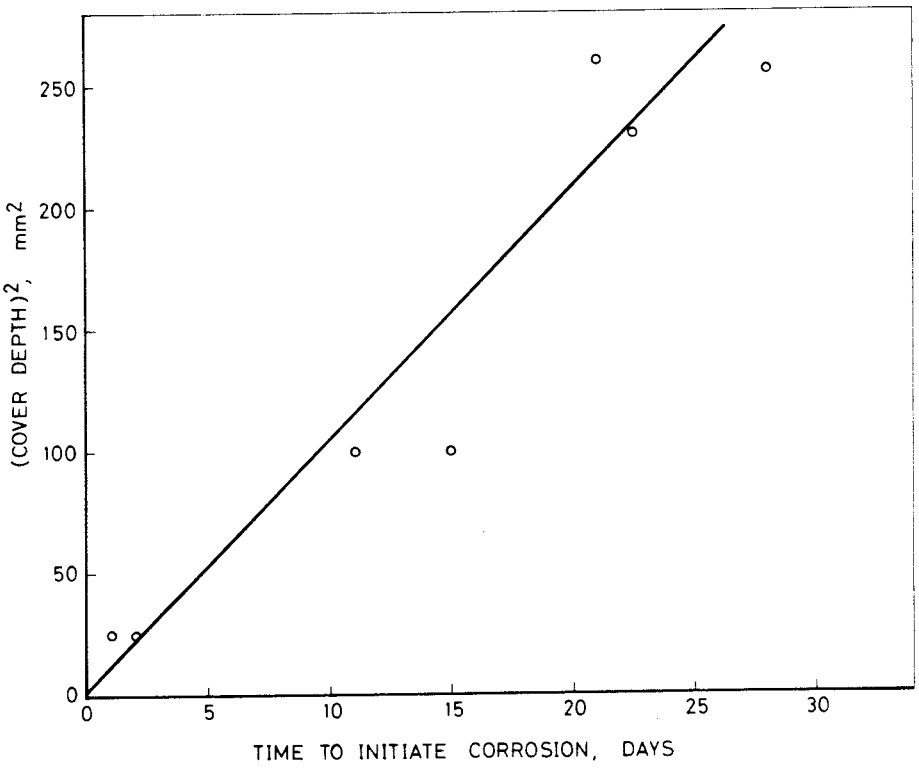

Fig. 21. The time of exposure to 1 M NaCl solution at 45°C and +100 mV SCE before the onset of corrosion plotted as a function of mortar cover depth.

The corrosion in the five-electrode sample was so rapid that the mortar cracked before the polarization data was taken. The sample is shown in Fig. 22. One of the electrodes with 5 mm cover in the five-electrode "Massiv" sample also began to corrode after approximately 3 weeks exposure to the chloride solution and is also shown in Fig. 22. The effect of the Cl ions on the electrochemical behaviour of single electrode samples is illustrated in Fig. 17. Whereas the steel in "Massiv" behaved as it did in anaerobic water, the steel embedded in "Standard" mortar rapidly began to corrode and its current density increased by >3 orders of magnitude. After completion of the polarization curves in Fig. 17, these samples were held at open circuit for two weeks and then again held at +100 mV SCE for four months. The current densities were then 4.0 and 100 A/m^2 for the "Standard" samples and $2.0.10^{-3}$ and $5.0.10^{-3}$ A/m^2 for the "Massiv" samples. These values indicate that chloride induced corrosion continues in the "Standard" samples but was not initiated in the "Massiv" samples after five months' exposure to the NaCl solution and an impressed anodic potential.

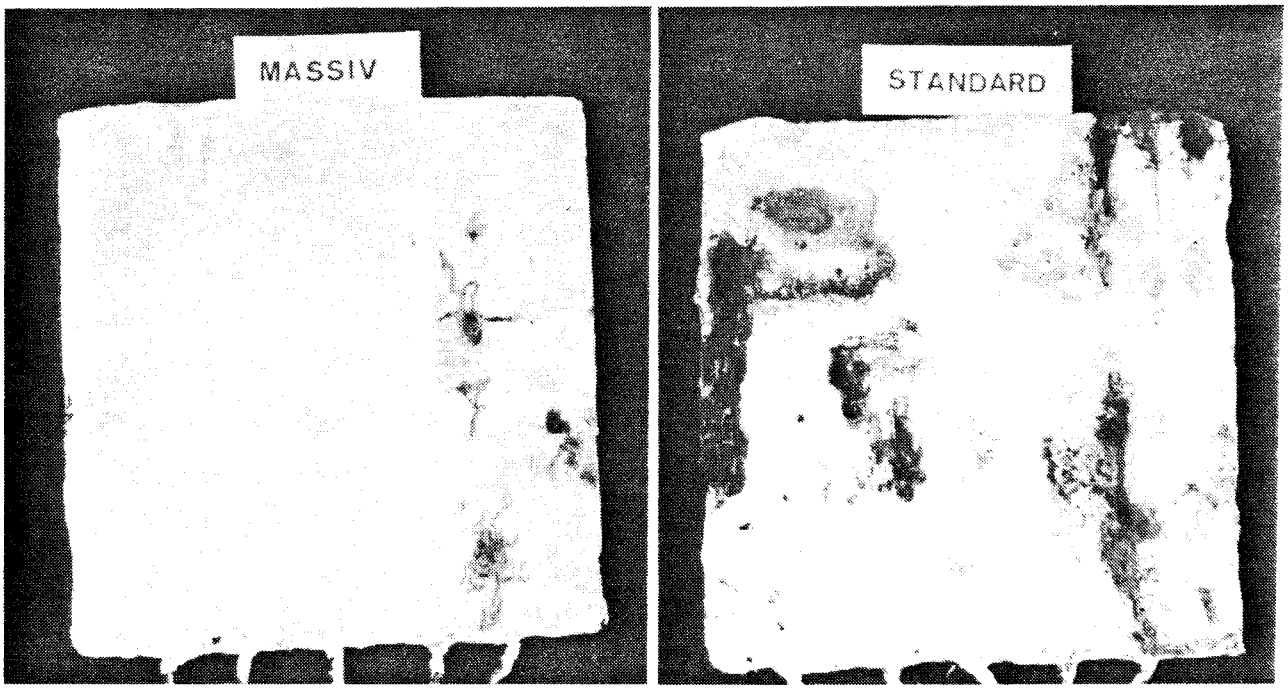

Fig. 22. Five-electrode samples of "Massiv" and "Standard" mortars after exposure to deaerated 1M NaCl solution at 45°C and +100 mV SCE for 4 weeks.

The effective diffusion coefficient, D, for chloride ions in "Standard" mortar can be calculated using the approximation of Fick's second Law:

$$x = 2\sqrt{Dt}$$

where x is the distance the ions have diffused in time t. The data in Fig. 20 give a value of $D = 260.10^{-13}\ m^2/s$. While this value falls within the range of data given in Table I for diffusion at 50 C, it probably represents a faster rate of diffusion because corrosion initiation is considered [17] to require a chloride concentration of the order of a few tenths a percent rather than the ppm levels detected in the diffusion experiment. Moreover, using the value of D from Table II and the above equation, chloride should not penetrate the 5 mm cover of the "Massiv" samples to a level of more than a few ppm within ~60 days whereas, in fact, corrosion of one electrode began after only ~20 days. The apparent discrepancy may be due to cracks in the mortar or to a difference in the diffusion characteristics of mortar relative to paste. The most probable reason, however, is the electric field introduced in the mortar by holding the electrode at an anodic potential. The negatively charged chloride ions would be attracted to the electrode by electrical forces in addition to the concentration gradient.

The electrochemical behaviour of samples held at 35°C was similar to that of samples held at 45°C but the chloride-induced corrosion was slower.

After two months in chloride solution at 35°C and +100 mV SCE some of the "Standard" samples had begun to corrode but several remained in the completely passive state, as indicated in Figs. 23 and 24. None of the "Massiv" samples had shown any indication of corrosion in this period.

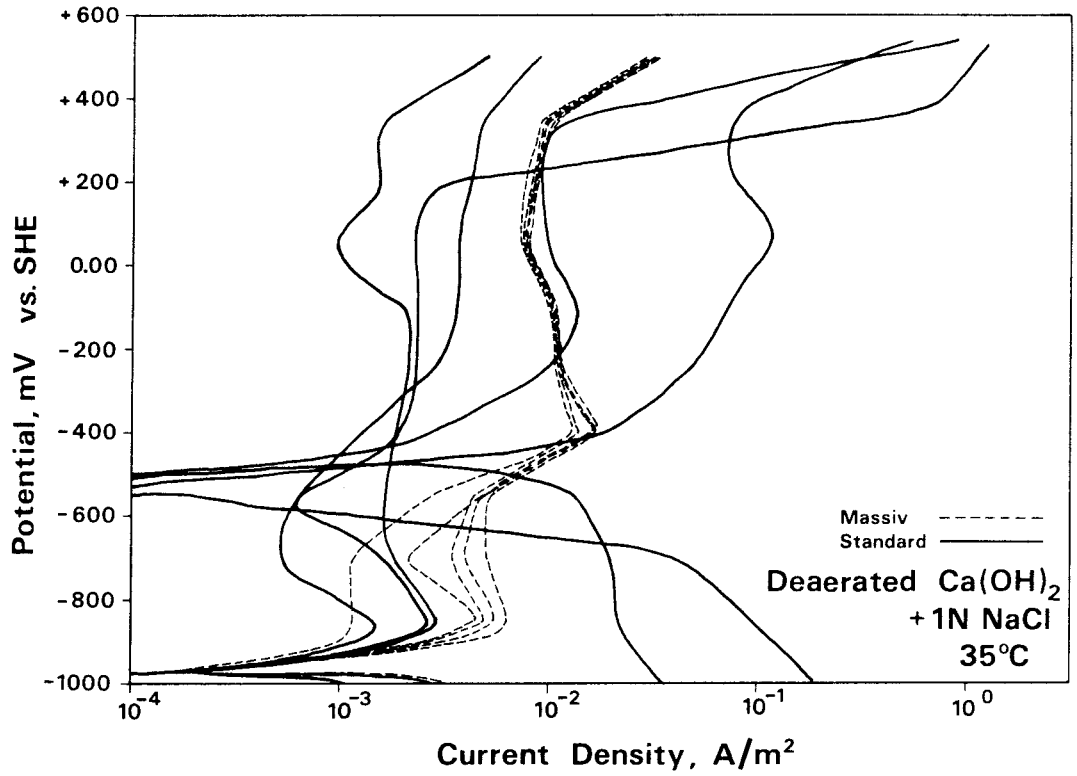

Fig. 23. Electrochemical potentiostatic polarization curves for one five-electrode sample each of "Massiv" and "Standard" mortar in dearated NaCl solution at 35°C.

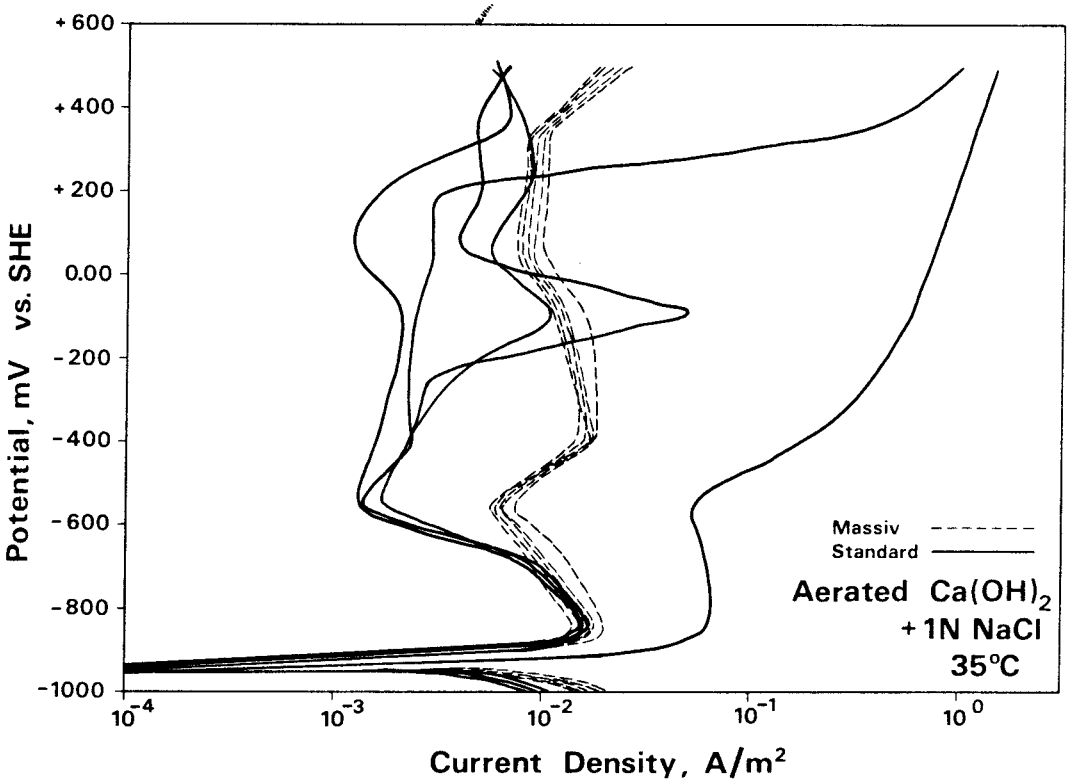

Fig. 24. Electrochemical potentiostatic polarization curves for one five-electrode sample each of "Massiv" and "Standard" mortar in aerated NaCl solution at 35°C.

CONCLUSIONS

Although "Massiv" cement has a higher non-chemically bound (evaporable) water content than has "Standard" cement, the water is present in a much finer pore structure. The physically dense structure of "Massiv" cement results in (a) a much higher electrical resistivity than that of the "Standard" cement and (b) significantly lower diffusion rate for chloride ions. The diffusivity data also indicate that "Massiv" cement reacts with the chloride ions to a greater extent than does the "Standard" cement.

The electrochemical measurements reveal several differences between the two cements:

(i) There is considerably less scatter in the data for "Massiv" samples than for "Standard" (or other cements that we have investigated). This presumably is also a result of the finer, more homogeneous structure of the "Massiv" cement.

(ii) In deaerated conditions, the steel embedded in "Massiv" mortar has a passive current density which is 10-100 times greater than that of steel in "Standard" mortar. This should not, however, be regarded as detrimental. It has the advantage that, in normal aerated structures buried underground, the available oxygen will be cathodically reduced more rapidly in "Massiv" concrete than in "Standard" concrete. The corrosion potential of "Massiv" will, therefore, fall more rapidly to a low level characteristic of deaerated structures which is well below that at which chloride ions can cause pitting corrosion.

(iii) The corrosion of steel in "Massiv" mortar is affected by the environment to a significantly lower extent than is steel in "Standard" mortar. Thus, while chloride ions rapidly initiate corrosion of the steel in "Standard" and give corrosion rates of $\sim$1-2 mm/yr. at a potential of +100 mV SCE, corrosion initiation is considerably slower in "Massiv" mortar and in that sample in which corrosion was initiated, the corrosion rate was $\sim$ 0.3 mm/yr. This difference is illustrated in Fig. 21. Similarly, "Massiv" mortar has a lower tendency to allow crevice corrosion: whereas such attack was observed in all "Standard" electrodes exposed to O_2 or CO_2 saturated water at 45°C and +100 mV SCE, it has not yet been observed in any of the "Massiv" samples.

In summary, it may be concluded that, for underground structures, steel in "Massiv" concrete will achieve a low corrosion potential characteristic of deaerated concrete more rapidly than will steel in "Standard" concrete. While there are no exact limits for the chloride attack (pitting being a function of potential, concentration and pH) it is not considered to be important at $E^{<}$-300 mV SCE in the high pH solution existing in concrete[18]. Consequently, it is not possible for chloride attack to occur at potentials low enough for hydrogen evolution at pressures >1 atm. (E<-1040 SCE). Thus, it is not possible to have chloride-initiated corrosion and corrosion-induced hydrogen evolution simultaneously. However, on the basis of this short term investigation, and a survey of published data of steel in anaerobic concrete, it is not possible to predict the exact value of the potential that the steel will achieve over a very long period of time.

ACKNOWLEDGEMENTS

We would like to express our gratitude to Inge L.H.Hansson, Laboratory of Applied Physics I, and Dirch H. Bager, Laboratory of Building Materials, at the Technical University of Denmark for their contribution to this study. We would also like to thank Robert F.M. Bakker of Stichting Betonresearch van de Nederlandse Cementindustrieen for helpful discussion of the work.

REFERENCES

1. B.Ost and G.E.Monfore, Journal of the PCA Research & Development Laboratories, 5, p.23 (1963)

2. F.S.Fulton, "The Properties of Portland Cements Containing Milled Granulated Blastfurnace Slag". A Portland Cement Institute Monograph, Johannesburg, South Africa (1974)

3. K.Tuutti, "Corrosion of Steel in Concrete - Effect of Cement Type". The Swedish Cement and Concrete Research Institute, Report No. 8157, 1981-11-20.

4. R.Bakker, "On the Cause of Increased Resistance of Concrete made from Blast Furnace Cement to the Alkali-Silica Reaction and to Sulphate Corrosion". Doctoral Thesis. Mining and Metallurgy Faculty, R.W.T.H. Aachen, 1980.

5. E.Hammond and T.D.Robson, The Engineer. 199, p.78 (1955)

6. O.E.Gjørv, Ø.Vennesland & A.H.S. El-Busardy, 9th Annual Offshore Technology Conference, Houston, Texas, p.581 (1979)

7. H.W.Whittington, I.McCarter and M.C.Forde, Magazine of Concrete Research, 33, p.48 (1981)

8. I.L.H.Hansson and C.M.Preece, to be published.

9. C.L.Page, N.R.Short and A.El Tarras, Cement and Concrete Research, 11, p.395 (1981)

10. E.J.Sellevold and D.H.Bager, Proc. 7th International Congress on the Chemistry of Cement, Paris, 1980, Vol. 4, p.394.

11. R.Bakker, private communication.

12. M.Pourbaix, "Atlas of Electrochemical Equilibria", Pergamon Press, Oxford (1966).

12a M.Pourbaix, Corrosion Science, 14 25 (1974)

13. H.Arup, "Corrosion/79", NACE, Houston, Texas. Paper No. 134 (1979)

14. P.Fidjestøl & N.Nilsen, "Steel in Concrete" No. 2, Jan. (1979) ed. H.Arup, Korrosionscentralen.

15. N.J.M. Wilkins & P.F.Lawrence, "Concrete in the Oceans", Techn. Report No. 6, Cement & Concrete Ass., U.K. (1980)

16. P.Longuet, L.Burglen and A.Zelwer, Revue de Materiaux de Construction, 676, p.35 (1973).

17. C.L.Page, Nature, 258, p.514 (1975)

18. M.Pourbaix, Corrosion, 26, p.431 (1970)

FÖRTECKNING ÖVER KBS TEKNISKA RAPPORTER

1977-78

TR 121 KBS Technical Reports 1 - 120.
Summaries. Stockholm, May 1979.

1979

TR 79-28 The KBS Annual Report 1979.
KBS Technical Reports 79-01--79-27.
Summaries. Stockholm, March 1980.

1980

TR 80-26 The KBS Annual Report 1980.
KBS Technical Reports 80-01--80-25.
Summaries. Stockholm, March 1981.

1981

TR 81-17 The KBS Annual Report 1981.
KBS Technical Reports 81-01--81-16
Summaries. Stockholm, April 1982.

1982

TR 82-01 Hydrothermal conditions around a radioactive waste repository
Part 3 - Numerical solutions for anisotropy
Roger Thunvik
Royal Institute of Technology, Stockholm, Sweden
Carol Braester
Institute of Technology, Haifa, Israel
December 1981

TR 82-02 Radiolysis of groundwater from HLW stored in copper canisters
Hilbert Christensen
Erling Bjergbakke
Studsvik Energiteknik AB, 1982-06-29

TR 82-03 Migration of radionuclides in fissured rock:
Some calculated results obtained from a model based on the concept of stratified flow and matrix diffusion
Ivars Neretnieks
Royal Institute of Technology
Department of Chemical Engineering
Stockholm, Sweden, October 1981

TR 82-04 Radionuclide chain migration in fissured rock -
The influence of matrix diffusion
Anders Rasmuson *
Akke Bengtsson **
Bertil Grundfelt **
Ivars Neretnieks *
April, 1982

* Royal Institute of Technology
Department of Chemical Engineering
Stockholm, Sweden

** KEMAKTA Consultant Company
Stockholm, Sweden

TR 82-05 Migration of radionuclides in fissured rock -
Results obtained from a model based on the concepts of hydrodynamic dispersion and matrix diffusion
Anders Rasmuson
Ivars Neretnieks
Royal Institute of Technology
Department of Chemical Engineering
Stockholm, Sweden, May 1982

TR 82-06 Numerical simulation of double packer tests
Calculation of rock permeability
Carol Braester
Israel Institute of Technology, Haifa, Israel
Roger Thunvik
Royal Institute of Technology
Stockholm, Sweden, June 1982

TR 82-07 Copper/bentonite interaction
Roland Pusch
Division Soil Mechanics, University of Luleå
Luleå, Sweden, 1982-06-30

TR 82-08 Diffusion in the matrix of granitic rock
Field test in the Stripa mine
Part 1
Lars Birgersson
Ivars Neretnieks
Royal Institute of Technology
Department of Chemical Engineering
Stockholm, Sweden, July 1982

TR 82-09:1 Radioactive waste management plan
PLAN 82
Part 1 General
Stockholm, June 1982

TR 82-09:2 Radioactive waste management plan
PLAN 82
Part 2 Facilities and costs
Stockholm, June 1982

TR 82-10 The hydraulic properties of fracture zones and tracer tests with non-reactive elements in Studsvik
Carl-Erik Klockars
Ove Persson
Geological Survey of Sweden, Uppsala
Ove Landström
Studsvik Energiteknik, Nyköping
Sweden, April 1982

TR 82-11 Radiation levels and absorbed doses around copper canisters containing spent LWR fuel
Klas Lundgren
ASEA-ATOM, Västerås, Sweden 1982-08-11

TR 82-12 Diffusion in crystalline rocks of some sorbing and nonsorbing species
Kristina Skagius
Ivars Neretnieks
Royal Institute of Technology
Department of Chemical Engineering
Stockholm, Sweden, 1982-03-01

TR 82-13 Variation in radioactivity, uranium and radium-226 contents in three radioactive springs and along their out-flows, northern Sweden
John Ek
Sverker Evans
Lennart Ljungqvist
Studsvik Energiteknik AB
Nyköping, Sweden, 1982-06-03

TR 82-14 Oral intake of radionuclides in the population
A review of biological factors of relevance for assessment of absorbed dose at long term waste storage
Lennart Johansson
National Defense Research Institute, Dept 4
Umeå, Sweden, October 1982

TR 82-15 Radioactive disequilibria in mineralised drill core samples from the Björklund uranium occurrence, northern Sweden
J A T Smellie
Geological Survey of Sweden
Luleå, December 1982

TR 82-16 The movement of a redox front downstream from a repository for nuclear waste
Ivars Neretnieks
Royal Institute of Technology
Stockholm, Sweden, 1982-04-19

TR 82-17 Diffusion of hydrogen, hydrogen sulfide and large molecular weight anions in bentonite
Trygve E Eriksen
Department of Nuclear Chemistry
Royal Institute of Technology, Stockholm
Arvid Jacobsson
Division of Soil Mechanics
University of Luleå
Sweden, 1982-07-02

TR 82-18 Radiolysis of ground water from spent fuel
Hilbert Christensen
Erling Bjergbakke
Studsvik Energiteknik AB
Nyköping, Sweden, 1982-11-27

TR 82-19 Corrosion of steel in concrete
Carolyn M Preece
Korrosionscentralen
Glostrup, Denmark, 1982-10-14

TR 82-20 Fissure fillings from Finnsjön and Studsvik, Sweden.
Identification, chemistry and dating
Eva-Lena Tullborg
Sven Åke Larson
Swedish Geological, Gothenburg
December 1982

TR 82-21 Sorption of actinides in granitic rock
B Allard
Department of Nuclear Chemistry
Chalmers University of Technology
Göteborg, Sweden 1982-11-20